

Synthesis and properties of selenium trihydride at high pressuresXiao Zhang,^{1,2} Wan Xu,^{1,2} Yu Wang,^{1,2} Shuqing Jiang,¹ Federico A. Gorelli,^{1,3,4} Eran Greenberg,⁵
Vitali B. Prakapenka,⁵ and Alexander F. Goncharov^{1,2,6}¹Key Laboratory of Materials Physics, Institute of Solid State Physics, Chinese Academy of Sciences, Hefei, 230031, China²University of Science and Technology of China, Hefei, 230026, China³Istituto Nazionale di Ottica, CNR-INO, 50019 Sesto Fiorentino, Italy⁴European Laboratory for Non Linear Spectroscopy (LENS), 50019 Sesto Fiorentino, Italy⁵Center for Advanced Radiation Sources, University of Chicago, Chicago, Illinois 60637, USA⁶Geophysical Laboratory, Carnegie Institution of Washington, Washington, DC 20015, USA

(Received 19 December 2017; revised manuscript received 4 February 2018; published 26 February 2018)

The chemical reaction products of molecular hydrogen (H_2) with selenium (Se) are studied by synchrotron x-ray diffraction (XRD) and Raman spectroscopy at high pressures. We find that a common H_2Se is synthesized at 0.3 GPa using laser heating. Upon compression at 300 K, a crystal of the theoretically predicted $Cccm$ H_3Se has been grown at 4.6 GPa. At room temperature, H_3Se shows a reversible phase decomposition after laser irradiation above 8.6 GPa, but remains stable up to 21 GPa. However, at 170 K $Cccm$ H_3Se persists up to 39.5 GPa based on XRD measurements, while low-temperature Raman spectra weaken and broaden above 23.1 GPa. At these conditions, the sample is visually nontransparent and shiny suggesting that metallization occurred.

DOI: [10.1103/PhysRevB.97.064107](https://doi.org/10.1103/PhysRevB.97.064107)**I. INTRODUCTION**

Hydrogen dominated compounds (superhydrides) are promising materials for the realization of high temperature superconductivity as they can combine the unique prerequisites for superconductivity such as high-frequency phonons, strong electron-phonon coupling, and a high density of the electronic states [1]. Numerous theoretical calculations support this idea and predict the superconducting transition temperatures in the range of 50–235 K for a variety of hydrides [2–9]. Recently, following a theoretical prediction [2] (see also [3]), a new record high T_C up to 203 K has been reported in the H-S system at 150 GPa [10]. This result confirms that high temperature superconductivity in hydride can be reached and also that theoretical calculations can be quite accurate in predicting novel hydrides and in estimating their T_C . The mechanism of superconductivity of the H-S system and its structural and compositional changes at high pressures were then explored extensively [11–21]. These studies have also stimulated significant interest in searching for new high- T_C superconductors in other dense hydride materials.

Selenium (Se) is adjacent and isoelectronic to sulfur in the periodic table. Since it has a larger atomic core and is weaker than S in electronegativity, it is possible that Se may exhibit a different chemistry. Nevertheless, it would be plausible to expect that selenium hydrides could also demonstrate high- T_C superconductivity. Therefore, its examination is of interest for comparison of the behavior of these two materials, which may be revealing for uncovering the mechanism of superconductivity. Two independent theoretical studies have been then performed on this subject with the result that selenium hydrides exhibit high T_C in the range of 40–131 K at megabar pressures [22,23].

Similarly to the H-S system, the highest T_C is predicted for the cubic $Im-3m$ structure of H_3Se and it is expected to be about 40% lower than that in H_3S . This prediction is still awaiting experimental confirmation. However, to understand the superconducting properties of selenium superhydrides (if any) it is of fundamental importance to investigate the synthesis conditions and determine their structural and electronic properties. Synthesis of H_2Se at ambient pressure and an elevated temperature has been reported previously [24].

High pressure as a general route to material synthesis [25] has been used in the past to obtain hydrides under thermodynamic equilibrium conditions [26–29]. This occurs due to modifications of the chemical bonds under pressure which can affect the compositions and properties of the stable compounds. One promising route to increase the hydrogen composition is via the mixing of molecular H_2S and H_2 that form a new molecular compound $(H_2S)_2H_2$ (that is H_3S , the stoichiometric ratio of H and S atoms is 3:1) at low pressures near 3.5 GPa [30]. In the case of the H-S system, it has been shown that a $Cccm$ H_3S [3] with similar structural and vibrational properties can be also synthesized at high temperatures (above 50 GPa or so) from molecular H_2 and H_2S as well as elemental H_2 and S, or by unloading (at 300 K) $Im-3m$ H_3S synthesized directly at high pressures [17] (see also [31]). Recently, the synthesis of a host-guest $(H_2Se)_2H_2$ compound, with stoichiometric ratio of H and Se atoms of 3:1, was reported at 4.2 GPa and room temperature [32]. According to this work, this compound decomposes into the constituent elements at 24 GPa and room temperature, so is H_2Se . Here we report the synthesis of $Cccm$ H_3Se at pressures as low as 4.6 GPa and show its structural stability (probed with XRD) up to 40 GPa if compressed at low temperatures while the Raman spectroscopy and visual observations suggest metallization

above 23 GPa. This behavior is similar to the vibrational and electronic properties of *Cccm* H₃S albeit at higher pressures.

II. EXPERIMENTAL METHODS

We performed the experiments in symmetric diamond anvil cells (DACs) equipped with anvils with central culets of 300 μm in diameter. Small pieces of Se were positioned in a hole in a rhenium gasket and filled with H₂ gas at ~ 200 MPa. The material of interest (H₃Se) has been synthesized in two steps. In the first step, we reacted H₂ and Se to form H₂Se. We gently laser heated Se using several tens of milliwatts of a 532 nm solid state laser (up to 400 mW in some experiments) sharply focused to a spot of 2–3 μm in diameter to melt it (monitored visually) at pressures lower than 0.5 GPa. At such low pressures we have made a mixture of H₂Se and H₂ fluids judging from the Raman spectra measured. To synthesize a H₃Se solid, we slowly compressed the fluids to about 5 GPa forming a single crystal (Fig. 1) [33]. Our room temperature experiments to 21.6 GPa yielded the results similar to those of [32], which report chemical decomposition at higher pressures. To avoid chemical reaction at room temperature, we thus cooled the sample down to 100–200 K and performed a further compression at low temperature. Low-temperature Raman measurements were performed in a continuous flow cryostat using liquid nitrogen with the DAC positioned in vacuum. Temperature was measured with Pt and Si resistance sensors attached to the DAC close to the sample. Pressure was controlled at low temperatures through the mechanical feedthroughs connected to four loading DAC screws. Two low-temperature Raman experiments have been performed at 200 K (experiment A) and 100 K (experiment B). The temperatures in the two low-temperature synchrotron XRD pressure runs were about 170 K created using a cryostream N₂ refrigerator [16,17]. Once the target pressure is reached, the sample was warmed up to room temperature and then decompressed.

Pressure was determined using the ruby fluorescence [34] and gold XRD [35] pressure markers with the appropriate temperature corrections. For the Raman experiments, a backscattering geometry was adopted for confocal measurements with incident laser wavelengths of 532 nm [36]. The Raman notch filters (three per each excitation wavelengths; additionally 488

and 660 nm laser lines were available) were of a very narrow bandpass (Optigrate) allowing Raman measurements down to 10 cm^{-1} in the Stokes and anti-Stokes. One of these notch filters is used as a beam splitter to inject the laser into the optical path. The XRD experiments were collected at the synchrotron beam line sector 13 (GSECARS) of the Advanced Photon Source (APS) of the Argonne National Laboratory with the wavelengths of 0.3344 \AA . The initial data reduction was performed using Dioptas software [37]. The lattice parameters were determined by a manual fitting of the observed XRD pattern to simulated diffraction patterns using PowderCell software [38]. These results were further refined using UnitCell software [39] (where possible).

III. RESULTS AND DISCUSSIONS

Raman spectra after laser heating at 0.3 GPa show a new sharp peak that appears at about 2350 cm^{-1} (Fig. 2). This peak can be assigned to the H-Se stretching mode [33], indicating synthesis of a fluid H₂Se. At 2.2 GPa, H₂Se crystalizes into a separate translucence solid, attaching on the rim of gasket and Se [red circles in the Fig. 1(a)]. At these conditions, a Raman peak of the H-Se stretching mode becomes broad and increases in intensity. A bulk liquid H₂ (solid above 5.5 GPa) phase remains coexistent in the high-pressure chamber conditions.

At 4.6 GPa, remarkably, a new crystal of a columnar habit grows up [Fig. 1(b)], similar to the observation of (H₂S)₂H₂ [30]. Please note that this crystal is grown in the vicinity of the solid H₂Se but in a slightly different location. In contrast to H₂Se, the Raman spectrum of H₃Se reveals a H₂ vibrational mode distinct in frequency of that of bulk H₂ (Figs. 2 and 3), signifying that this compound exhibits a mixed molecular H₂Se-H₂ structure, where the H₂ molecules are slightly elongated.

At 7 GPa, XRD diffraction peaks match well the theoretically predicted *Cccm* structure of H₃Se [22] (Fig. 4). Please note that the XRD image clearly shows that there are two sets of diffraction rings: spotty (larger crystallites) and quasicontinuous ones. The latter ones originate from unreacted Se remaining in the cavity. In contrast, the rings of H₃Se are all spotty, indicating that the newly crystallized H₃Se consists of rather large grains. In the second XRD experiment at low temperatures to 39.5 GPa, where we examined a very small sample of about 3 μm in width, we demonstrated that this single crystal habit persists to quite high pressures and *Cccm* H₃Se remains stable to the highest pressure reached (Fig. 5).

The unit cell volume (at 170 K) versus pressure results represent a smooth curve which we have been able to fit with a single Vinet equation of state (EOS) with the following parameters: $V_0 = 56(4) \text{\AA}^3$, $K_0 = 9.3(2.6) \text{GPa}$, $K_0' = 4.7(5)$ (Fig. 6). The data for room-temperature experiments in *Cccm* H₃S and H₃Se are shown for comparison. Apart from a small temperature (in H₃Se [32]) and both temperature and compositional (in H₃S [17]) shifts, the EOSs are very similar. However, no direct comparison of the EOS parameters can be made, because the room temperature values are not reported.

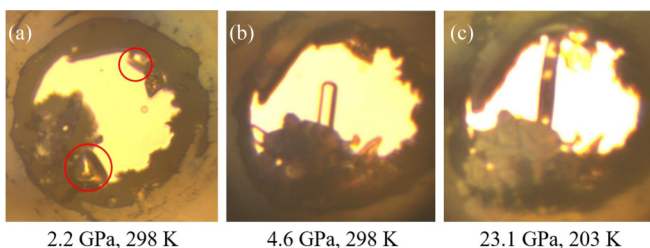


FIG. 1. Microphotographs of the DAC cavities at elevated pressures demonstrating the formation of H-Se compounds. (a) Solid H₂Se is grown (circled). (b) *Cccm* H₃Se is grown pictured as a bar in the middle of the cavity. (c) Supposedly a metallic H₃Se is formed; the crystal bridged the cavity sides and deformed. It reflects light in the areas where the surface is perpendicular to the optical axis and is dark (nontransparent for the transmitted light) where it is tilted.

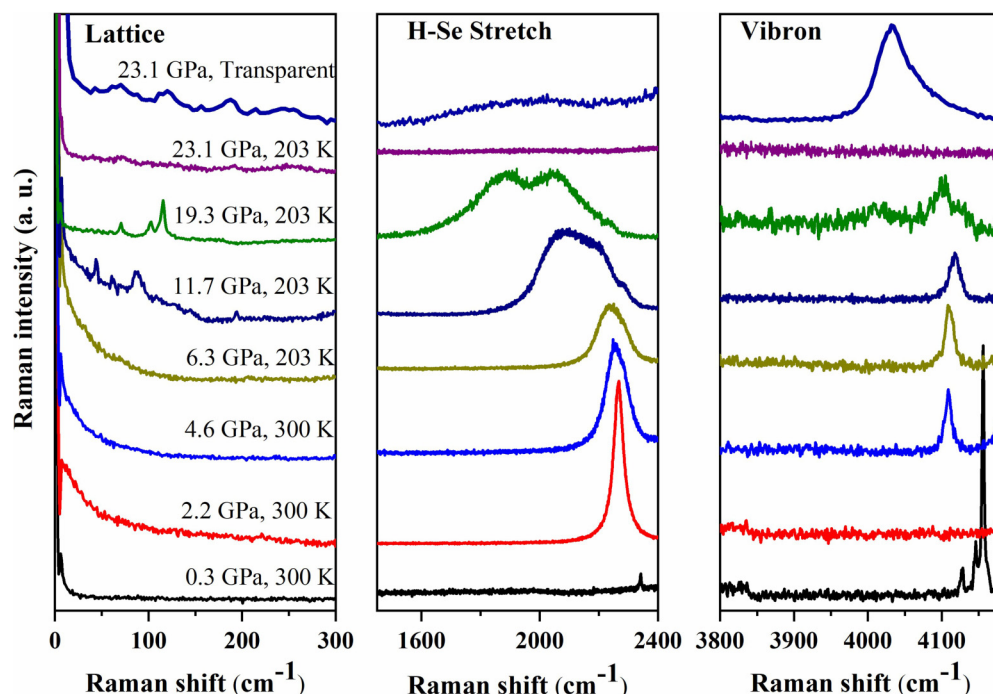


FIG. 2. Raman spectra of H-Se compounds at different pressures and temperatures in experiment A. Please note the vibron modes (a triplet) of bulk unreacted H_2 at 0.3 GPa. At higher pressures they become a single band shifting to higher frequencies outside the presented frequency range.

In contrast to the low-temperature stability, at room temperature H_3Se crystals show signs of instability at elevated

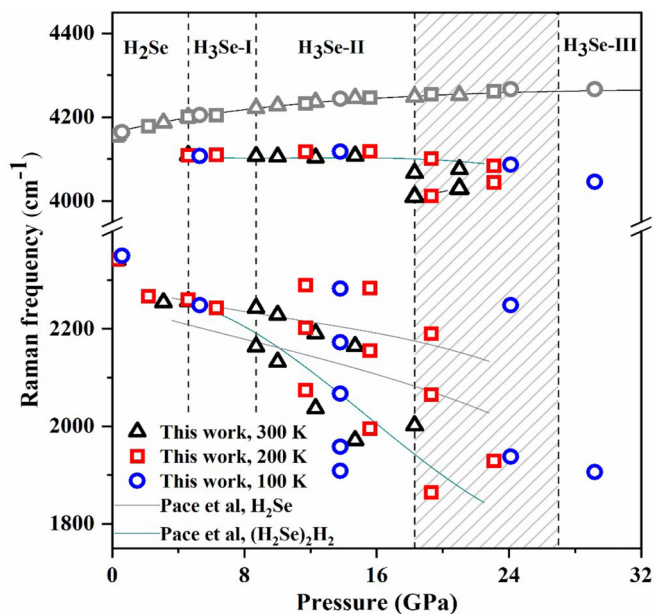


FIG. 3. The pressure dependence of the Raman frequencies of H-Se compounds as a function of pressure at 300 K and in the low-temperature experiments A and B emphasizing the difference in vibrational properties of the H_3Se compound compared with H_2Se , H_2 , and $(\text{H}_2\text{Se})_2\text{H}_2$ at room temperature [32]. The black, blue, and red symbols correspond to the Raman bands observed in the H_2S and H_3S compounds at 300, 200, and 100 K, respectively. The gray symbols are the spectral positions of the bulk unreacted H_2 vibron; a solid line through these data is the literature data for H_2 [40].

pressures and temperatures revealing the disappearance of the characteristic Raman peaks after exposing the compound to a laser beam (Fig. 7). It is interesting that these peaks can be seen again after some time suggesting that the compound recrystallizes. In agreement with the results of a recent study [32], we find that *Cccm* H_3Se chemically decomposes above 21 GPa confirmed through the observations of irreversible disappearance of the Raman bands above 21.6 GPa (Fig. 8). These

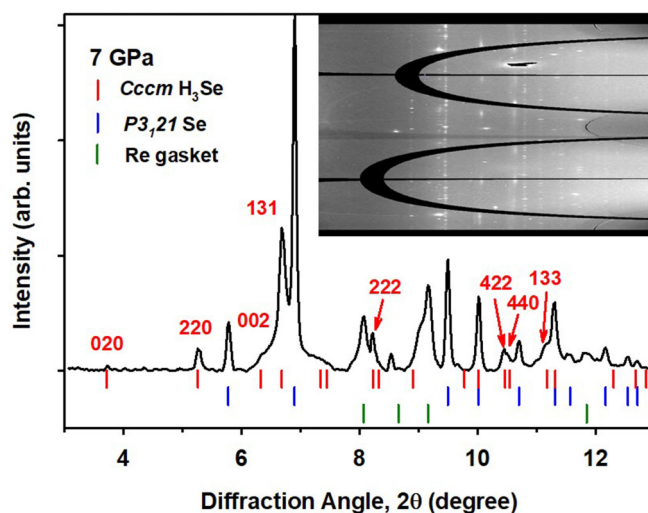


FIG. 4. XRD pattern of the H-Se compound at 7.0 GPa and 300 K. The x-ray wavelength is 0.3344 Å. Red vertical ticks with the peak indexing are presented for the *Cccm* H_3Se [22] and blue vertical ticks - for Se-I [41]. The gasket is made of Re. The inset is a two-dimensional diffraction image in the radial coordinates (cake).

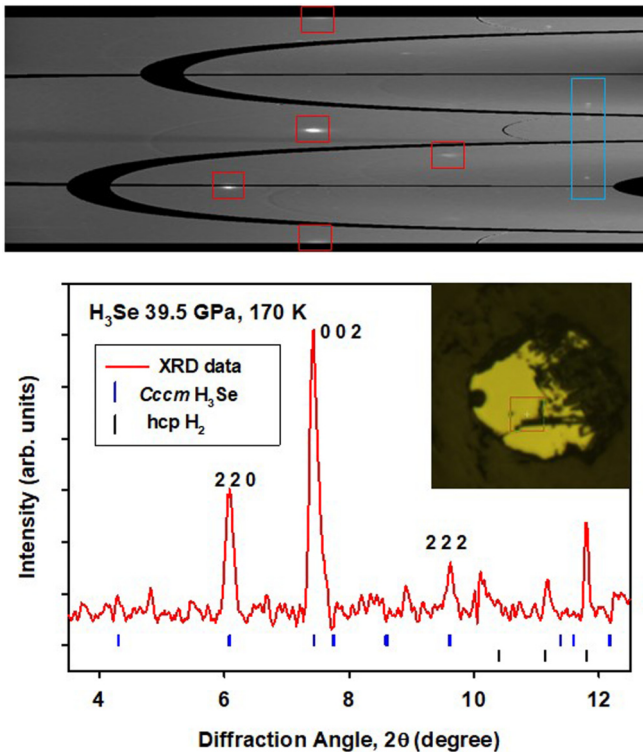


FIG. 5. XRD of a single-crystal like H_3Se at 39.5 GPa. The x-ray wavelength is 0.3344 Å. The bottom panel is the integrated one-dimensional pattern. The blue ticks indicate the peak positions of the predicted $Cccm$ H_3Se (the values of a and b lattice parameters are indistinguishable) and the black ticks of hcp hydrogen (phase I). The inset shows a microphotograph of the sample before cooling; the red square has a side of approximately 20 μm . The top panel is a two-dimensional diffraction image in the radial coordinates (cake), the single crystal spots of the sample are marked by red squares and those of bulk H_2 by the blue rectangle. Please note that in this low-temperature experiment we could only rotate the sample within ± 2 deg because of a cryostream nozzle attached to the DAC, limiting the number of observed reflections.

observations are broadly in agreement with the investigations of H_2S which shows various x-ray and visible light induced instabilities, especially at room temperature [16,42–44].

When compressed at low temperatures, at 11.7 GPa the Raman spectra of H_3Se show the H-Se stretching mode broadens due to splitting into several components (Fig. 2). This is similar to the observations of [17,30] in H_3S . Concomitantly, several new Raman peaks appear below 200 cm^{-1} . These changes suggest that a molecular ordering occurs in the $Cccm$ H_3Se -II modification (Fig. 3) that result in the emergence of the well-structured Raman spectra revealing the libron and translational modes at low frequencies and splitting of the fundamental intramolecular modes (likely via the crystal field). The behavior of the H-Se stretching and lattice modes is more complex in the lower temperature experiment B (Figs. 3 and 9). There are five clear peaks in the Se-H stretching region at 13.8 GPa. Moreover, the bending modes can be found at about 1000 cm^{-1} above 13.8 GPa at 100 K (marked as red arrows in Fig. 9). These peaks are close in frequency to higher order

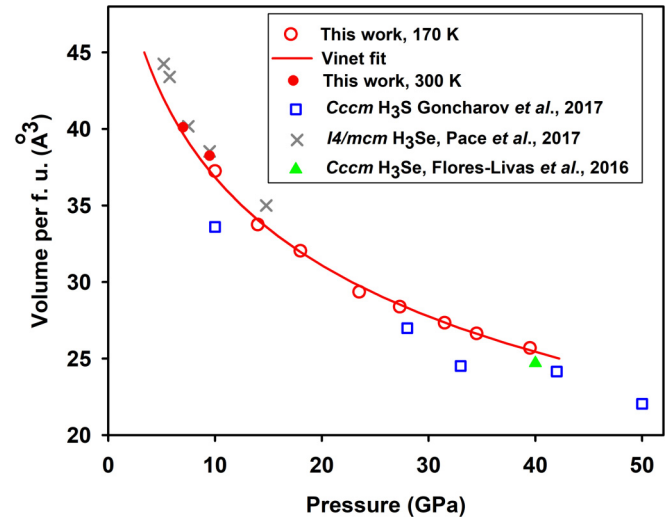


FIG. 6. Equation of state of $Cccm$ H_3Se at 170 K of this work in comparison to that of experiment at room temperature [32] and theory [22] and also to the EOS of $Cccm$ H_3S at 170 K [17]. The error bars are within the symbol dimensions.

roton modes of bulk H_2 , so they are difficult to single out at higher temperature and lower pressures.

Further compression results in a second major change in the vibrational spectra of $Cccm$ H_3Se III (Figs. 2 and 3). Beginning at 19.3 GPa, the H_2 vibron mode of $Cccm$ H_3Se shows a redshift. In addition, at 19.3 GPa we observed a visual change in the sample appearance: a part of the transparent crystal in the center of the chamber turns black and opaque after laser irradiation. However, the Raman spectra are indistinguishable between these two different regions. Above 23 GPa, the H-Se stretching modes turn into a single broad band; concomitantly

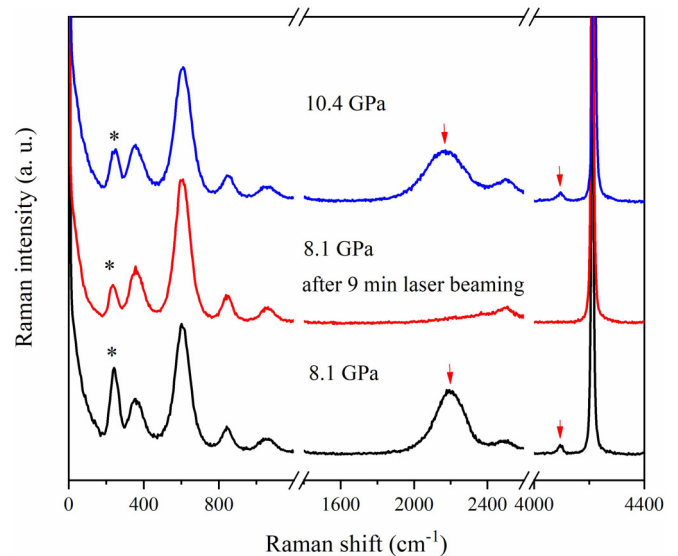


FIG. 7. Decomposition and recovery of H_3Se at 300 K revealed by the disappearance and appearance back again of the Raman peaks of the compound (marked by the red arrows). The asterisk (*) indicates the peak of Se. The Raman peaks of the surrounding bulk hydrogen remain unaffected.

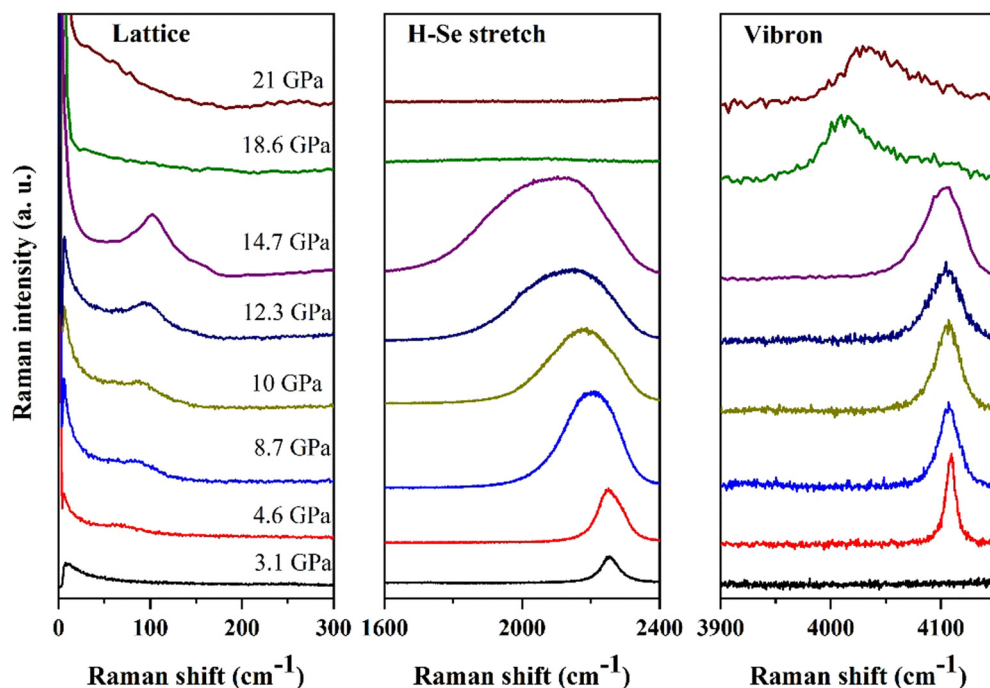


FIG. 8. Raman spectra of H-Se compounds at elevated pressures at room temperature. The excitation wavelength is 532 nm.

the lattice and the H_2 vibron mode also broaden. At 23.1 GPa, the whole crystal becomes nontransparent and shiny in some regions where, we assume, its surface is perpendicular to the optical axis so it can reflect the incoming light back [Fig. 1(c)]. Remarkably, the Raman spectra of this state did not yield any measurable signal (likely due to an abrupt decrease in the laser penetration depth) except one spot where a broad-

ened H_2 vibron and H-Se stretching band could be observed (Fig. 2).

The transition is shifted to a higher pressure at 100 K (compared to that at 200 K) where the crystal is still transparent at 24.1 GPa and abrupt changes in the Raman spectra have been observed at higher pressures. In experiment B at 100 K, we have been able to observe weak and broad Raman spectra

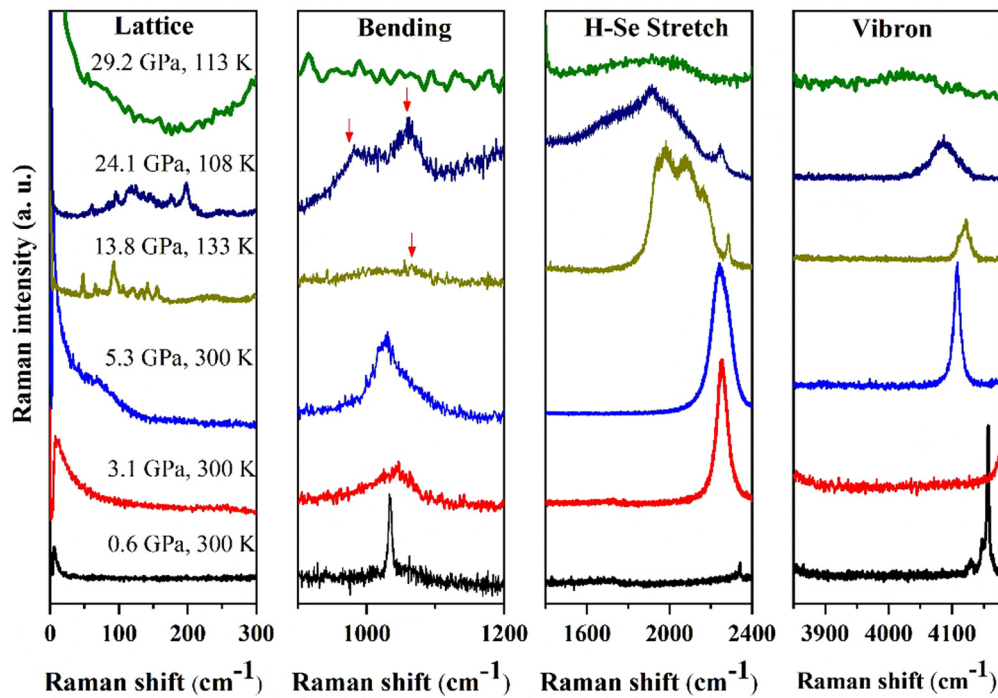


FIG. 9. Raman spectra of H-Se compounds at different pressures and temperature in experiment B. The excitation wavelength is 532 nm. As in Fig. 2, please note the vibron modes of bulk H_2 at 0.6 GPa. At higher pressures they become a single band shifting to higher frequencies outside the presented frequency range. The red arrows mark the positions of the Se-H bending mode.

up to 29 GPa. The transition into this supposedly metallic phase does not depend on whether we expose the sample to the laser radiation, since the observed weak spectra at 29.1 GPa in experiment B suggest that the transformation (observed visually) occurred without any laser irradiation. It is interesting that we have been able to observe the signs of this transition even at 300 K at 18.6 GPa through an abrupt redshift, appearance of asymmetry, and broadening of the H_2 vibron mode (Figs. 8 and 9). The Raman band asymmetry can be tentatively assigned to a coupling of the phonon mode with a continuum due to charge carriers, which is common for doped semiconductors and bad metals (e.g., [45]).

While the Raman and visual observations at 100 and 200 K suggest possible structural and electronic changes above 21 GPa, synchrotron XRD patterns obtained at 170 K over this pressure range showed no clear indication of a structural change (Figs. 5 and 6). All the sample patterns measured at these pressures could be indexed to the *Cccm* structure, and no obvious discontinuity was observed in the EOS. *Cccm* H_3Se has slightly larger lattice parameters and unit cell volume than H_3S [17,30], which seems plausible due to the larger dimension of Se ion compared to S. The unit cell volume which we measured also agree well with the theoretical predictions for *Cccm* H_3Se at 40 GPa [22] and the results of the recent experiments at 300 K to lower pressures [32]. Thus, our Raman, visual, and XRD observations suggest that the most plausible explanation of the transformation above 23 GPa at low temperatures is metallization via band gap closure. Please note that the theoretical calculations of [3] suggest a semiconducting behavior of *Cccm* H_3S in the whole pressure stability range, while no calculations are reported on the band gap of *Cccm* H_3Se . The existence of three distinct regimes in high-pressure behavior, which include orientationally disordered, orientationally ordered, and metallic, has been also reported in *Cccm* H_3S based on the Raman experiments [17]. The discrepancy between the experiment and theory concerning the electronic structure of H_3Se and H_3S is puzzling and requires further investigation.

The reported here peculiar behavior of the low-temperature Raman spectra contrasts a recent report on the synthesis of $(H_2Se)_2H_2$ [32], which, consistently with our study, points

out its chemical instability above 24 GPa albeit at 300 K. We comment that the Se-H system behaves similarly to the S-H one in that it shows chemical instability to decomposition at room temperature [16,42–44], while at low temperatures there is no decomposition creating the path to the superconducting state [10] via a crossover in chemical composition.

IV. SUMMARY

Our experiments show rich physical and chemical transformations detected with XRD and Raman spectroscopy. The demonstration of the synthesis of *Cccm* H_3Se at 4.6 GPa and its stability to 40 GPa at 170 K paves the way to study the properties of this material at higher pressures, where the superconductivity is predicted. The changes in properties of this material with pressure including a possible metallization at 23 GPa are very much in line with the behavior of *Cccm* H_3S . Our results suggest that the H-Se system may be promising for reaching high- T_C superconductors at lower pressures than in the H-S system.

ACKNOWLEDGMENTS

This work was supported by National Natural Science Foundation of China under Grants No. 21473211, No. 11674330, No. 11604342, No. 11504382, and No. 51727806, Science Challenge Project No. TZ2016001. A.F.G. was supported by the Chinese Academy of Sciences visiting professorship for senior international scientists (Grant No. 2011T2J20) and Recruitment Program of Foreign Experts. GSECARS is supported by the US NSF (EAR-1128799, DMR-1231586) and DOE Geosciences (DE-FG02-94ER14466). Use of the APS was supported by the DOE-BES under Contract No. DEAC02-06CH11357. We thank Mario Santoro, Maddury Somayazulu, Eugene Gregoryanz, and Xia-Jia Chen for useful comments and suggestions. We thank Nicholas Holtgrewe for the excellent technical support at GSECARS. We thank Yu-Sheng Chen (ChemMatCARS) for help with a cryostream N_2 refrigerator. We also thank the anonymous referee for sharing with us the results of unpublished calculations of the electronic band structure of H_3Se .

-
- [1] N. W. Ashcroft, *Phys. Rev. Lett.* **92**, 187002 (2004).
 [2] Y. Li, J. Hao, H. Liu, Y. Li, and Y. Ma, *J. Chem. Phys.* **140**, 174712 (2014).
 [3] D. Duan, Y. Liu, F. Tian, D. Li, X. Huang, Z. Zhao, H. Yu, B. Liu, W. Tian, and T. Cui, *Sci. Rep.* **4**, 6968 (2014).
 [4] X. Zhong, H. Wang, J. Zhang, H. Liu, S. Zhang, H. F. Song, G. Yang, L. Zhang, and Y. Ma, *Phys. Rev. Lett.* **116**, 057002 (2016).
 [5] H. Wang, J. S. Tse, K. Tanaka, T. Iitaka and Y. Ma, *Proc. Natl. Acad. Sci.* **109**, 6463 (2012).
 [6] H. Liu, I. I. Naumov, R. Hoffmann, N. W. Ashcroft, and R. J. Hemley, *Proc. Natl. Acad. Sci.* **114**, 6990 (2017).
 [7] Y. Li, G. Gao, Y. Xie, Y. Ma, T. Cui, and G. Zou, *Proc. Natl. Acad. Sci.* **107**, 15708 (2010).
 [8] I. A. Kruglov, A. G. Kvashnin, A. F. Goncharov, A. R. Oganov, S. Lobanov, N. Holtgrewe, S. Jiang, V. Prakapenka, E. Greenberg, and A. V. Yanilkin, [arXiv:1708.05251v2](https://arxiv.org/abs/1708.05251v2).
 [9] A. Shamp and E. Zurek, in *Novel Superconducting Materials* (De Gruyter, Poland, 2017), Vol. 3, p. 14.
 [10] A. P. Drozdov, M. I. Erements, I. A. Troyan, V. Ksenofontov, and S. I. Shylin, *Nature (London)* **525**, 73 (2015).
 [11] N. Bernstein, C. S. Hellberg, M. D. Johannes, I. I. Mazin, and M. J. Mehl, *Phys. Rev. B* **91**, 060511(R) (2015).
 [12] D. A. Papaconstantopoulos, B. M. Klein, M. J. Mehl, and W. E. Pickett, *Phys. Rev. B* **91**, 184511 (2015).
 [13] I. Errea, M. Calandra, C. J. Pickard, J. Nelson, R. J. Needs, Y. Li, H. Liu, Y. Zhang, Y. Ma, and F. Mauri, *Phys. Rev. Lett.* **114**, 157004 (2015).

- [14] Y. Quan and W. E. Pickett, *Phys. Rev. B* **93**, 104526 (2016).
- [15] R. Akashi, M. Kawamura, S. Tsuneyuki, Y. Nomura, and R. Arita, *Phys. Rev. B* **91**, 224513 (2015).
- [16] A. F. Goncharov, S. S. Lobanov, I. Kruglov, X. M. Zhao, X. J. Chen, A. R. Oganov, Z. Konopkova, and V. B. Prakapenka, *Phys. Rev. B* **93**, 174105 (2016).
- [17] A. F. Goncharov, S. S. Lobanov, V. B. Prakapenka, and E. Greenberg, *Phys. Rev. B* **95**, 140101(R) (2017).
- [18] L. P. Gor'kov and V. Z. Kresin, *Sci. Rep.* **6**, 25608 (2016).
- [19] M. Einaga, M. Sakata, T. Ishikawa, K. Shimizu, M. I. Erements, A. P. Drozdov, I. A. Troyan, N. Hirao, and Y. Ohishi, *Nat. Phys.* **12**, 835 (2016).
- [20] L. Ortenzi, E. Cappelluti, and L. Pietronero, *Phys. Rev. B* **94**, 064507 (2016).
- [21] T. Jarlborg and A. Bianconi, *Sci. Rep.* **6**, 24816 (2016).
- [22] J. A. Flores-Livas, A. Sanna, and E. K. U. Gross, *Eur. Phys. J. B* **89**, 63 (2016).
- [23] S. Zhang, Y. Wang, J. Zhang, H. Liu, X. Zhong, H. F. Song, G. Yang, L. Zhang, and Y. Ma, *Sci. Rep.* **5**, 15433 (2015).
- [24] J. Rawling and J. Toguri, *Can. J. Chem.* **44**, 451 (1966).
- [25] P. F. McMillan, *Nat. Mater.* **1**, 19 (2002).
- [26] V. V. Struzhkin, D. Y. Kim, E. Stavrou, T. Muramatsu, H. K. Mao, C. J. Pickard, R. J. Needs, V. B. Prakapenka, and A. F. Goncharov, *Nat. Commun.* **7**, 12267 (2016).
- [27] T. Scheler, M. Marques, Z. Konopkova, C. L. Guillaume, R. T. Howie, and E. Gregoryanz, *Phys. Rev. Lett.* **111**, 215503 (2013).
- [28] C. M. Pepin, A. Dewaele, G. Geneste, P. Loubeyre, and M. Mezouar, *Phys. Rev. Lett.* **113**, 265504 (2014).
- [29] Z. Geballe, H. Liu, A. K. Mishra, M. Ahart, M. Somayazulu, Y. Meng, M. Baldini, and R. J. Hemley, *Angew. Chem.* **130**, 696 (2018).
- [30] T. A. Strobel, P. Ganesh, M. Somayazulu, P. R. C. Kent, and R. J. Hemley, *Phys. Rev. Lett.* **107**, 255503 (2011).
- [31] B. Guigue, A. Marizy, and P. Loubeyre, *Phys. Rev. B* **95**, 020104 (2017).
- [32] E. J. Pace, J. Binns, M. Pena Alvarez, P. Dalladay-Simpson, E. Gregoryanz, and R. T. Howie, *J. Chem. Phys.* **147**, 184303 (2017).
- [33] B. A. Paldus, S. A. Schlueter, and A. Anderson, *J. Raman Spectrosc.* **23**, 87 (1992).
- [34] D. D. Ragan, R. Gustavsen, and D. Schiferl, *J. Appl. Phys.* **72**, 5539 (1992).
- [35] O. L. Anderson, D. G. Isaak, and S. Yamamoto, *J. Appl. Phys.* **65**, 1534 (1989).
- [36] A. F. Goncharov, *Int. J. Spectrosc.* **2012**, 617528 (2012).
- [37] C. Prescher and V. B. Prakapenka, *High Press. Res.* **35**, 223 (2015).
- [38] W. Kraus and G. Nolze, *J. Appl. Crystallogr.* **29**, 301 (1996).
- [39] T. J. B. Holland and S. A. T. Redfern, *Mineral. Mag.* **61**, 65 (1997).
- [40] H.-k. Mao and R. J. Hemley, *Rev. Mod. Phys.* **66**, 671 (1994).
- [41] R. Keller, W. Holzapfel, and H. Schulz, *Phys. Rev. B* **16**, 4404 (1977).
- [42] Y. Li, L. Wang, H. Liu, Y. Zhang, J. Hao, C. J. Pickard, J. R. Nelson, R. J. Needs, W. Li, Y. Huang, I. Errea, M. Calandra, F. Mauri, and Y. Ma, *Phys. Rev. B* **93**, 020103 (2016).
- [43] M. Sakashita, H. Fujihisa, H. Yamawaki, and K. Aoki, *J. Phys. Chem. A* **104**, 8838 (2000).
- [44] H. Fujihisa, H. Yamawaki, M. Sakashita, A. Nakayama, T. Yamada, and K. Aoki, *Phys. Rev. B* **69**, 214102 (2004).
- [45] F. Cerdeira, T. A. Fjeldly, and M. Cardona, *Phys. Rev. B* **8**, 4734 (1973).